applied sciences

MDPI

Article

Metronidazole-Loaded Porous Matrices for Local Periodontitis Treatment: In Vitro Evaluation and In Vivo Pilot Study

Dorota Kida [1], Bożena Karolewicz [1,*], Adam Junka [2], Aleksandra Sender-Janeczek [3], Irena Duś [4], Dominik Marciniak [1] and Małgorzata Szulc [3]

1 Department of Drug Form Technology, Wroclaw Medical University, Borowska 211 A, 50-556 Wroclaw, Poland; dorota.kida@umed.wroc.pl (D.K.) dominik.marciniak@umed.wroc.pl (D.M.)
2 Department of Pharmaceutical Microbiology and Parasitology, Wroclaw Medical University, Borowska 211 A, 50-556 Wroclaw, Poland; adam.junka@umed.wroc.pl
3 Department of Periodontology, Wroclaw Medical University, Krakowska 26, 50-425 Wroclaw, Poland; aleksandra.sender-janeczek@umed.wroc.pl (A.S.-J.); malgorzata.szulc@umed.wroc.pl (M.S.)
4 Department of Oral Pathology, Wroclaw Medical University, Krakowska 26, 50-425 Wroclaw, Poland; irena.dus-ilnicka@umed.wroc.pl
* Correspondence: bozena.karolewicz@umed.wroc.pl; Tel.: +48-71-784-03-15

Received: 3 September 2019; Accepted: 22 October 2019; Published: 25 October 2019



Abstract: Periodontal therapy focuses on thorough removal of subgingival calculus and plaque products followed by the smoothing out of root surfaces. However, such conventional mechanotherapeutic approaches are inefficient with regard to microbial biofilm elimination from the space between the root and deep periodontal pockets. Therefore, local chemotherapeutic agents need to be applied. Local antimicrobial treatment is also considered a safer treatment, as it avoids systemic complications related to drug application. In this study, porous matrices consisting of gelatin (GE) and cellulose derivatives (carboxymethylcellulose (CMC) and hydroxyethyl cellulose (HEC)) were loaded with antimicrobial drug metronidazole (MTZ). The matrices' structural morphology, physiochemical properties, swelling and degradation ratio, mechanical properties, and MTZ release from the matrices were analyzed. Additionally, cytotoxicity tests for fibroblast and osteoblast cell cultures (L929 and U2-OS, respectively) and antimicrobial activity assessments of MTZ-loaded matrices against anaerobic Bacteroides sp. Bacteria were performed. Finally, clinical application of HEC matrices into periodontal pockets was conducted. The applied matrices showed a high antibacterial efficacy and a moderate cytotoxicity in vitro. The clinical application of HEC dressings corresponded with the decrease of periodontal pockets' depth and bleeding observed 1 month after a single application. The presented results show that intra-pocket application of metronidazole using manufactured matrices may serve not only as a support for a standard treatment in periodontal practice but also as an alternative to systemic drug administration in this setting. Clinical data were analyzed using a nonparametric Friedman's ANOVA for dependent trials.

Keywords: metronidazole; cellulose derivatives; periodontal; clinical pilot study

1. Introduction

The main purpose of periodontal treatment is to protect and regenerate diseased periodontal tissues. Another aim of such treatments is to stop chronic inflammatory processes destroying periodontal tissue and leading to pathological pocket formation. The basic method of periodontal infection treatment, referred to as scaling and root planning (SRP), relies on the elimination of subgingival bacterial deposits from the tooth surface by mechanical removal of the plaque [1,2]. However, this approach has limitations, mostly due to the inability of dental hand instruments to reach areas

affected by infection and due to the requirement for a highly skilled operator. As a result, SRP does not guarantee the elimination of anaerobic bacteria residing in the base of deep periodontal pockets as well as in the interstitial spaces, from where they are able to migrate into the tissues [2,3]. The relationship between periodontal surgery treatment and sepsis caused by the dissemination of bacteria through the bloodstream is already well established [4–7]. Therefore, to ensure efficient removal of pathogenic microorganisms from difficult-to-access sites, local antimicrobial therapy is applied [2,8,9]. Unfortunately, oral administration may lead to insufficient concentration of the drug within the periodontal pocket and to the rise of bacterial resistance against the compound [10]. Answering an urgent clinical demand, local drug-delivery devices have been developed to provide a high concentration of antimicrobial compound directly to the infected site. This minimizes systemic exposure to the drug [11,12] and limits any potential adverse reactions [13].

Helpfully, due to its topography, a periodontal pocket may serve as a storage of an antimicrobial agent that can be released continually from the carrier, providing an anti-infectious measure in the proximity of the affected site [14]. Studies show that local use of metronidazole in the treatment of periodontal disease enhances the therapeutic effect of SRP but that the use of the metronidazole is associated with a lower risk of tissue damage, dental hypersensitivity, or colonization as a result of microbial migration from the interstitial spaces inaccessible to the surgeon [1,8]. Thus, the choice of an appropriate carrier for drug delivery is of paramount importance to achieving a favorable outcome. Presently, a wide spectrum of carriers, both organic and inorganic, are employed for this purpose, with gelatin and cellulose (or its derivatives) being the most prominent examples.

Gelatin is a natural protein obtained by partial hydrolysis of collagen. It possesses several beneficial features, including supporting cell proliferation and differentiation, and favorable physical-chemical attributes such as adhesiveness, plasticity, biocompatibility, biodegradability, water solubility, and the ability to form stable gels [15–17]. Gelatin-based matrices are currently used in tissue engineering as drug carriers (providing agents promoting bone regeneration) and as dressings in wound treatment. Gelatin/polymeric porous hydrogels are oxygen-permeable and have the ability to absorb tissue exudates and to create a moist environment, which is required for efficient tissue healing [18,19]. Examples of cellulose-derived carriers include carboxymethyl cellulose (CMC) and hydroxyethyl cellulose (HEC), which are biodegradable, water-soluble cellulose ethers, displaying plasticizing muco-adhesive properties. To enhance the efficiency of carrier compounds, two or more polymers can be used as substrates and matrix properties can be adjusted to the desired parameters [20–22]. Mixtures of cellulose derivatives and natural polymers, i.e., gelatin, are used in dressings for the treatment of chronic wounds [23–25]. Moreover, freeze-drying of such gels, polymer dispersions, or their mixtures leads to the formation of dry dressings displaying a porous structure of a large surface area. Additionally, it has been shown that such lyophilized formulations are more stable then semi-solid formulations [20].

The aim of this study was to design, perform, and evaluate porous matrices with regard to their use as supportive agents or as an alternative approach to periodontal pocket local treatment. For this purpose, we prepared carriers, which consisted of the biocompatible polymer gelatin (GE) and of cellulose derivatives carboxymethylcellulose sodium salt (CMC) and hydroxyethyl cellulose (HEC). We loaded these carriers with metronidazole (MTZ) chemotherapeutic, known for its antimicrobial effect against microorganisms colonizing and in infecting periodontal pockets [13]. We hypothesized that MTZ incorporated into matrices and delivered directly into periodontal pockets would provide good support in periodontal treatment.

2. Materials and Methods

2.1. Matrix Preparation

The porous metronidazole-loaded (Amara, Poland) matrices were generated using freeze-drying technique. Firstly, dispersion of each polymer was separately prepared in water using a mechanical

stirrer (L366, Labinco BV, Breda, The Netherland), with rotation speed adapted to the viscosity of the dispersions. The 3% carboxymethyl cellulose sodium salt (25–75 mPa·s, Serva, Germany) and 3% (w/w) hydroxyethyl cellulose (3400–5000 mPa·s, Aldrich Chemical Co., Sheboygan Falls, WI, USA) dispersions were prepared at room temperature, while the 20% (w/w) type A porcine gelatin (Avantor Performance Materials Poland S.A., Gliwice, Poland) solution was prepared at 60 °C. The matrices were sealed overnight in a refrigerator to ensure clear, bubble-free solutions equilibrated to room temperature. Next, glycerol and MTZ (Sigma, Neustadt an der Weinstraße, Germany) were added to obtain the concentrations listed in Table 1. The mixture was homogenized by whip mixing at 2340 rpm (Gako e/s, Eprus, Bielsko-Biala, Poland) to get a stable foam; 2.0 g of each mixture was poured in a cylindrical plastic mold with a diameter of 30 mm and thickness of 5 mm. The foamed mixtures were frozen at −15 °C for 36 h and then freeze-dried at room temperature with ultimate vacuums of 9×10^{-2} to 1.3×10^{-1} mBar (Lyovac GT2, Steris, Köln, Germany) for 12 h. The dried sponges were stored in tightly sealed containers in the fridge until use.

Table 1. Composition of metronidazole (MTZ)-loaded matrices. GE—gelatin, CMC–carboxymethyl cellulose sodium salt, HEC—hydroxyethyl cellulose, GLY—glycerol, MTZ—metronidazole.

Batch Code	GE	CMC	HEC	GLY	MTZ
	(mg per matrix)				
CMC1	72.0	43.2	-	180.0	19.8
CMC2	144.0	32.4	-	180.0	19.8
CMC3	216.0	21.6	-	180.0	19.8
HEC1	72.0	-	43.2	180.0	19.8
HEC2	144.0	-	32.4	180.0	19.8
HEC3	216.0	-	21.6	180.0	19.8

2.2. Physical Properties of Matrix

The fabricated matrices were evaluated for thickness, mass, and drug content uniformity. Drug content uniformity, between batches and within batches, was determined by dissolving individually weighed matrices (n = 6) in water in a volumetric flask. The obtained solutions were filtered through a G-2 glass filter (40 µm). An aliquot of the filtrate was suitably diluted and analysed for MTZ content using UV spectrophotometer (Jasco V650 PC, Tokyo, Japan) at 320-nm wavelength. The thickness of the matrices was measured at six randomly selected spots with a screw gauge. For mass uniformity, 20 inserts from each batch were weighed individually and their average mass was determined. The acceptable deviation of particular matrix mass compared to average matrix mass was established as 5%.

2.2.1. Surface Morphology Observation

The external surface of the dried matrices was observed under stereo zoom microscope (Opta View 7, Opta–Tech, Warszawa, Poland) under 10× objective at a zoom factor of 4× and the final magnification 40×. Images were digitized at 1280 × 1024 pixels.

2.2.2. Swelling Ratio and Degradation Weight Loss Analysis

The water-absorbing capacity of the dressings was determined in water using a gravimetric method. Dry matrices were accurately weighted (W) and then fixed on the tip of a needle. The dressings were then placed in a beaker containing 20 mL of distilled water at room temperature for 2 min. The weights of the beaker were recorded directly before immersing the matrix (W_0) and after pulling it out of the medium W_t. The percentage swelling ratio (SR) was calculated six times using Equation (1) as the ratio of the amount of the water absorbed by the matrix ($W_0 - W_t$) relative to the initial weight (W).

$$SR\% = ((W_0 - W_t)/W) \times 100 \quad (1)$$

The weight loss (% degradation, R%) of the matrices was calculated six times using the following Equation (2):

$$R\% = ((R_1 - R_2)/R_1) \times 100 \quad (2)$$

where R_1 and R_2 are the initial weight and the weight determined after the immersion of dry samples in artificial saliva solution at 37 ± 0.5 °C, horizontal shaking for 2 h, and drying. The simulated solution was composed of carboxymethyl cellulose sodium salt (4.4 g), NaCl (0.38 g), KCl (0.54 g), $CaCl_2$ (0.0065 g), $MgCl_2.6H_2O$ (0.02 g), D-sorbitol (Sigma, Germany) (13.5 g), KH_2PO_4, (0.06 g), and $Na_2HPO_4{\cdot}2H_2O$ (0.15 g) in 450.0 mL of distilled water.

2.2.3. Mechanical Properties Testing

Texture profiles of formulations including elongation at break and force at break were determined using a TA-XT plus texture analyzer (Stable Micro System, Britain) in a simple tension mode at ambient temperature. The samples in the form of circular patches of 30 mm in diameter were held by two clamps (Type A/TG, Stable Micro System, Britain) positioned at a distance of 2 mm (ILB). The higher clamp serving as a probe was forced up at a defined rate of 1 $mm{\cdot}s^{-1}$ to a defined distance of 50 mm and then driven down at a higher rate of 10 $mm{\cdot}s^{-1}$ until it reached the starting position. The force and elongation were measured until the matrix broke. From the resultant force–distance curve, maximum elongation at break (IL) as the distance to the positive peak and force at break as positive peak of the formulations were calculated using the Texture Exponent 32 software. The matrices were equilibrated in sealed molds at room temperature 20 min before testing. The maximum elongation (E) before the break of the matrices was established by the application of Equation (3):

$$E\% = (ILB/IL) \times 100 \quad (3)$$

2.3. In Vitro Metronidazole Release Studies

In vitro drug release studies were carried out using the FPX Apparatus type 1 (Vankel VK7025, Varian Inc., United States) [26]. The matrices were drowned in 500.0 mL of MQ water maintained at a temperature of 37 ± 0.5 °C and stirred at a speed of 50 rpm. Sink condition was maintained for the entire experiment. Aliquots of 3 mL were withdrawn at 5, 10, 15, 20, 30, 45, 60, 75, 90, and 120 min. The collected samples were filtered, and the drug content in each sample was analyzed after suitable dilution at λ = 320 nm using the ultraviolet-visible spectrophotometer (Jasco V650 PC, Japan). MQ water was used as the blank sample. The amount of MTZ released from the matrices was determined by back-calculating from the achieved data against a predetermined calibration curve of MTZ in MQ water.

Drug Release Kinetics

The drug release kinetics from the fabricated matrices were evaluated using the first-order kinetic model $\ln Q = \ln Q_0 - k{\cdot}t$ and the zero-order kinetic model equation $Q = Q_0 - k{\cdot}t$, where Q is the amount of drug released, k is the release constant, and *t* is time. Further, the data was fitted to Higuchi's Equation $Q = k{\cdot}\sqrt{t}$, where Q is the amount of drug released, *k* is the release constant, and *t* is time, and to Korsmeyer–Peppas' power law equation $Q = k{\cdot}t^n$, where Q is the fraction of the drug released in time t, k is the structural and geometric constant, and *n* is the release exponent.

2.4. Preparation of Extract for Cell Viability Assay

Extracts were prepared according to ISO 10,993 standards: Biological evaluation of medical devices; Part 5: Tests for in vitro cytotoxicity; and Part 12: Biological evaluation of medical devices, sample preparation and reference materials (ISO 10993-5:2009 and ISO/IEC 17025:2005). Briefly, MTZ-loaded matrices were manufactured as described, with the difference that this process took place directly in the wells of a 24-well plate (Nunc, Roskilde, Denmark) in a laminar chamber to maintain aseptic

conditions. Next, the dressings were immersed in 2 mL of sterile DMEM medium and incubated for 24–48 h at 37 °C/5% CO_2 (Binder, Tuttlingen, Germany). After incubation, the extracts were used in a cytotoxicity assay.

Cytotoxicity Assay of MTZ-Loaded Matrices Toward Fibroblast and Osteoblast Cell Cultures

The evaluation of potential cytotoxic effect displayed by the analysed formulations was tested using fibroblast and osteoblast reference cell cultures [27–29] (L929 and U2-OS, respectively) (ATCC, Manassas, VA, USA). Cells were incubated in a cell culture flask (Nunc, Roskilde, Denmark) at 37 °C/5% CO_2 in DMEM medium supplemented with 10% bovine serum (Sigma-Aldrich, Hamburg, Germany). When the cultures reached confluence, the cells were detached from the flask surface using trypsin/EDTA. Next, the suspended cells were centrifuged (400× *g* for 5 min); the cells were then resuspended in fresh DMEM medium. Cells were then counted using a Brucker chamber, and 100 µL of 10^5 cfu/mL of cell suspension was plated in a well of a 24-well plate. The cells were incubated for 24 h at 37 °C/5% CO_2. Next, the medium was removed, and previously prepared extracts (please refer to the preparation of extract section of this manuscript) were introduced to the cells. The samples were then incubated for the 24 h at 37 °C/5% CO_2 conditions. After incubation, the medium was removed and 100 µL of Neutral red (NR) dye (40 µg/mL; Sigma-Aldrich, Hamburg, Germany) was introduced to the wells of the plate. The cells were incubated with NR for 2 h at 37 °C. After incubation, the dye was removed and the wells were rinsed with PBS (Sigma Aldrich, Hamburg, Germany) and left to dry at room temperature. Subsequently, 150 µL of a destain solution (50% ethanol 96%, 49% deionized water, 1% glacial acetic acid; POCH) was introduced to each well. The plate was vigorously shaken in a microtiter plate shaker for 30 min until NR was extracted from the cells and formed a homogenous solution. Next, the value of NR absorbance was measured spectrometrically using a microplate reader (Multi-scan GO, Thermo Fisher Scientific, Waltham, MA, USA) at 540-nm wavelength. The absorbance value of the cells not treated with extracts was considered 100% of potential cellular growth (positive control).

2.5. Metronidazole Disk Diffusion Test

Microbial anaerobic strain of Bacteroides sp. used for the evaluation of metronidazole disk diffusion test from matrices was a part of the Strain Collection of Department of Pharmaceutical Microbiology and Parasitology of Wroclaw Medical University. The aforementioned strain was cultured on Schaedler agar plates (BioCorp, Frankfurt, Germany) at 37 °C in anaerobic conditions provided by GasPack bag (BD, Franklin Lakes, NY, USA). To assess the metronidazole diffusion, antimicrobial activity of the dressings was tested. In this purpose were aseptically cut out holes of 5-mm diameters using cork-borer in a fresh Schaedler medium. Next, the holes were filled with dressing fragments also 5 mm in diameter. At the same time, a fresh *Bacteroides* suspension of 2MF (established densitometrically) was prepared and cultured immediately on the Schaedler plate. Next, the plates were incubated at 37 °C in anaerobic conditions for 24 h. After incubation, a growth inhibition zone around the dressing was measured using a ruler as performed in routine inhibition zone assessments in the antibiotic disc diffusion method.

2.6. Clinical Pilot Study

The protocol of the study, informed consents, and the subject's information sheets were approved by the local research ethic committee (Bioethical Commission at the Medical University of Wroclaw) (decision number KB 98/2016): ClinicalTrials.gov Identifier: NCT03791099.

Clinical assessment was performed on the selected matrix based on hydroxyethyl cellulose (HEC2) according to the protocol (Figure 1). Twenty-three generally healthy patients were qualified for the study (14 women and 9 men, average age of 51). Enrollment started in April 2018, lasted three months, and finished in July 2018. Patients were divided into two groups—the test group (8 women and 4 men) and control group (6 women and 5 men). The patients had been treated at

Wroclaw University Department of Periodontology for periodontitis (stadium 2 or 3, grade B) [30]. In each group, fifteen periodontal pockets were examined. The selected patients were nonsmokers and had not taken any antibiotics (applied generally or locally) for the past 6 months. The patients had ≥2 interproximal sites with CAL ≥ 6 mm (not on same tooth) and ≥1 interproximal site with PD ≥ 5 mm. In order to rate the oral cavity hygiene, Approximal Plaque Index (API by Lange et al. (1977)) was used and plaque presence in interproximal sites was evaluated [31]. To assess the gum inflammation, the Bleeding on Probing (BOP by Ainamo and Bay (1975)) index was used [32]. Gum inflammation intensity was assessed with the use of the Papilla Bleeding Index (PBI, Saxer and Muhlemann (1975)), [33]. Periodontal tissue degradation was assessed by the measurement of periodontal pockets depth (PPD, probing pocket depth) and by the measurement of clinical attachment level (CAL). The probing was carried out with the use of a calibrated 1-mm periodontal probe (PCP UNC-15; Hu-Friedy, Chicago, IL, USA). Six measurement points were marked: mesio-buccal, buccal (i.e., mid-buccal), disto-buccal, mesio-palatal, palatal (i.e., mid-palatal), disto-palatal (upper jaw), mesio-lingual, lingual (i.e., mid-lingual), and disto-lingual (lower jaw). Periodontal examination was performed by one trained and calibrated periodontist (M.S.) at baseline and at follow-up time points. Calibration was performed on 10 patients who were not recruited to the study. Examiner reliability was high with agreement in assessment on all clinical parameters above 85%. The clinical examination was performed three times. On the first (qualification) visit, the output indicators were defined. During the first visit, a subgingival ultrasonic scaling was performed. For every patient, the deepest periodontal pocket was identified and, in the test group, metronidazole in polymer matrix was applied to the selected periodontal pocket, as shown in Figure 2. There was no application of the matrix in the control group.

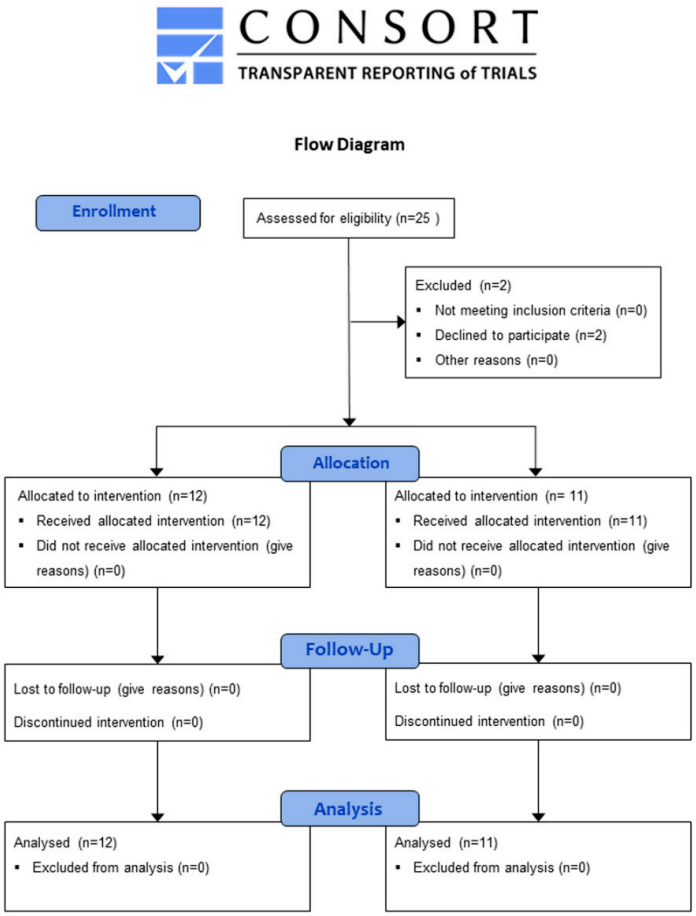


Figure 1. Structure flowchart of the clinical assessment of metronidazole-loaded matrix (HEC2).



Figure 2. Application of metronidazole-loaded matrix (HEC2) to periodontal pocket.

Two control tests of periodontal indices were carried out one week and one month following application [34,35]. During each visit the samples from selected, deepest periodontal pockets were collected (one in every patient) in order to check the existence of Porphyromonas gingivalis DNA, the bacteria of which is known as major periodotopathic bacterium [36]. After drying the site and isolation from saliva, a sterile paper point was inserted into the pocket for 10 s, then transferred to a sterile Eppendorf tube, and sent to the laboratory. Molecular biology was carried out in the Laboratory of Scientific Research of Molecular Biology, Department of Pathology, Oral Faculty of Dentistry. Genomic DNA from clinical specimens was obtained by a modified cetrimonium bromide (CTAB) method [37,38]. Every paper point taken from the gingival pockets was stored at −20 °C. During DNA isolation, they were placed in a 1.5-mL Eppendorf tube and 100 µL of sterile water was added and stirred in a vortex apparatus. Next, 70 µL of 10% sodium dodecyl sulfate (SDS) and 50 µL proteinase K at a concentration of 1 mg/mL (Sigma Aldrich, St. Louis, Missouri, USA) was added and stirred with vortex and, afterwards, incubated in Biorad T-100 thermocycler for 10 min at 65 °C. After this step, 100 µL of NaCl (5 M) and 100 mL of CTAB/NaCl (0.274 M CTAB (Hexadecyl trimetyloammonium bromide, 0.877 M NaCl, Sigma Aldrich) were added to each tube, vortexed gently, and incubated for 10 min at 65 °C. Next, extraction with chloroform (chloroform: Isoamyl Alcohol mixture 24:1, Fluka Analytical) and precipitation with isopropanol (2-propanol ≥99% Sigma-Aldrich) were performed. After 30 min of incubation, the material was incubated at −20 °C to precipitate, DNA was centrifuged 30 min at 12,000 rpm, the supernatant was decanted, the DNA pellet was dried at room temperature, and finally 100 µL of water (Sigma Aldrich) was added to each tube. The isolated DNA was stored at −20 °C. The PCR reaction used to amplify *Porphyromonas gingivali* genomic DNA is described in detail by Radwan-Oczko et al. [39]. The PCR reaction products were subjected to gel electrophoresis; products at a size of 405 base pairs were considered positive.

2.7. Statistical Analyses

The obtained experimental data were based on statistical interval scales. Normality of distributions for these variables was evaluated by three different statistical tests: Kolmogorov–Smirnov test, Lilliefors test, and Shapiro–Wilk test at the significance level $p = 0.05$. The homogeneity of variance was evaluated by the Levene and Brown–Forsyth tests at a set significance level of $p = 0.05$. The statistical significance of the differences between the two means was assessed—in the case of the lack of significance of tests for normality of the distribution—by the parametric t-test for independent samples or by the parametric Cochran–Cox test for unequal variances. In the case of variables that did not meet the normality of distribution criterion, the difference between the two means was evaluated by the nonparametric Mann–Whitney U test. For comparison of more than two means, depending on the results of normality tests of distributions and homogeneity of variances, parametric ANOVA algorithms or its nonparametric counterpart ANOVA Kruskal–Wallis together with the median test were used. In all the tests assessing the statistical significance of differences between means, the significance level

was assumed $p = 0.05$. In the case of obtaining statistically significant differences between the means in the ANOVA analysis, post hoc comparisons were made with the NIR test and the Scheffe test. Clinical data were analyzed using a nonparametric Friedman's ANOVA for dependent trials. The results in this manuscript are presented according to the scheme mean value (SR) ± standard error (SE). Statistical analyzes were performed using the STATISTICA PL® version 13.1 software.

3. Results

3.1. Physical Properties of Matrices

In the case of all formulations used, the incorporated drug content was higher than 87%. This high value confirms the efficacy of the technology applied. The higher the gelatin concentration, the higher the weight of the CMC and HEC matrices obtained (Table 2). The thickness of the CMC and HEC matrices (obtained from the same composition of particular substances) differed due to variations in the viscosity of these polymers. We observed that the high viscosity of a polymer correlated with lower porosity, resulting in matrices of lower thickness (Table 2).

Table 2. Thickness, mass, and drug content of matrices.

Batch Code	Drug Content in Matrices ± SE (%) n = 6	Mass of Matrices ± SE (g) n = 20	Thickness of Matrices ± SE (mm) n = 6
CMC1	96.307 ± 1.104	0.3495 ± 0.0017	2.02 ± 0.02
CMC2	92.410 ± 0.939	0.3885 ± 0.0013	2.98 ± 0.03
CMC3	104.445 ± 1.304	0.4147 ± 0.0006	3.05 ± 0.05
HEC1	99.993 ± 0.699	0.3159 ± 0.0015	1.01 ± 0.02
HEC2	91.669 ± 1.022	0.3785 ± 0.0030	2.06 ± 0.03
HEC3	90.600 ± 0.780	0.4181 ± 0.0013	2.10 ± 0.03

3.1.1. Morphological Observation of Surface

For this analysis, HEC and CMC-based matrices of different viscosity were selected. The color of all the obtained materials was white, and the material structure was soft and porous (Figures 3 and 4).

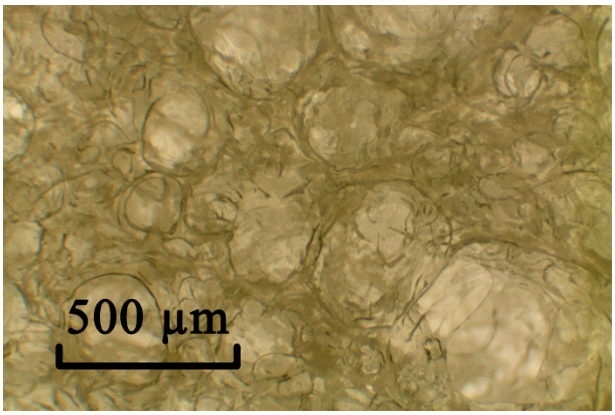


Figure 3. Morphology of the upper surface of CMC2 matrix, zoom 40×.

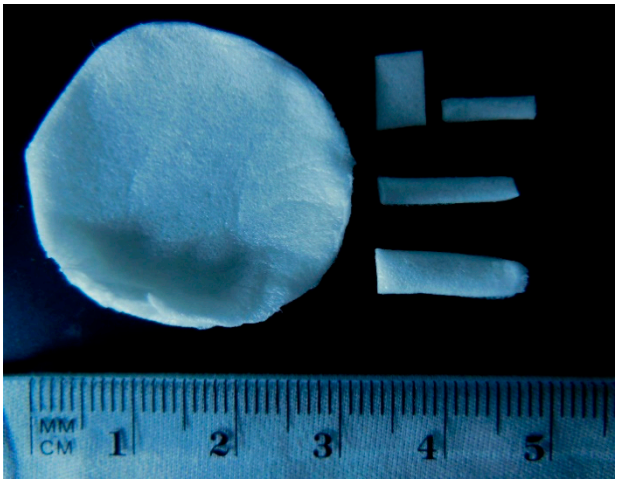


Figure 4. Optical image of CMC2 matrix directly before application (picture taken with Nikon S9300 camera using macro lens).

The materials obtained from each formulation were of various volumes due to the distinct composition of the polymers. Increasing gelatin concentrations resulted in denser and thicker dry matrices (CMC3 and HEC3). Higher concentrations of CMC and HEC produced a loosely formed polymeric network with a low number of holes, while the application of higher concentrations of gelatin correlated with denser, more homogenous porous structures produced that with a high number of small holes. Pore size increased along with increasing concentrations of CMC and HEC. The matrices with the same concentration of CMC and HEC showed similar physical properties and porosity. This indicates that matrix structure does not depend directly on the viscosity of the cellulose derivatives but more on the chemical structure of the polymer applied. The morphology of a porous structure plays an important role in its water-related properties.

3.1.2. Swelling Ratio and Degradation Weight-Loss Analysis

Swelling behavior of dry porous matrices is shown in Figure 5.

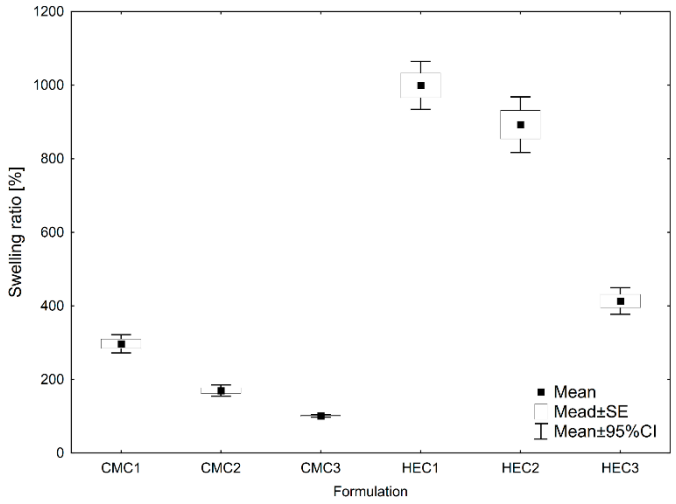


Figure 5. Swelling behavior of CMC and HEC porous matrices: Data are presented as the mean ± SE, n = 6.

Water uptake capacity is strongly affected by polymer concentration and morphology of the porous network of the matrices. Due to higher concentration of gelatin, these matrices were tighter and displayed poor water absorption. When a plasticizer was added, CMC and HEC films were able to absorb higher amounts of water and the variation trend was similar and correlated to the pore size.

The highest swelling value was achieved in systems containing HEC in its structure due to the presence of a high number of hydroxyl groups. Inside of gelatin macromolecules, numerous short-range interactions occur (including structure-stabilizing hydrogen bonds) that limit polymer's swelling and solubility [17,40]. Therefore, the addition of gelatin to the dispersion resulted in a reduction of absorbency.

Dried HEC matrices absorbed water corresponding to 1–3 times (100, 170, and 297%) their mass, while in the case of CMC matrices, the water uptake was significantly higher and reached 413, 893, and 999% of dried matrix mass, respectively. The swelling or water uptake ability defines the rate of body fluid (e.g., blood and saliva) uptake into the matrix and is one of the key factors determining its applicability in periodontal surgical treatment. We observed that the CMC matrix degradation ratio is lower than that of the HEC matrix, possibly due to the differing content of hydrophilic groups in these cellulose derivatives. Moreover, matrices with a higher CMC and HEC content displayed higher resistance to dissolution and higher swelling ability (Table 3). It is important to note that, in a periodontal setting, degradable matrices are of high applicability as their use eliminates the necessity of removal by surgical means and allows new tissue to grow and proliferate. A statistically significant difference was observed between all formulations with CMC and HEC (parametric ANOVA test, $p < 0.05$) with regard to all parameters presented above.

Table 3. Weight loss analysis of CMC and HEC porous matrices: Data are presented as the mean ± SE, n = 6.

Batch Code	Weight Loss of Matrices ± SE (%) n = 6
CMC1	11.58 ± 1.83
CMC2	20.89 ± 2.55
CMC3	27.83 ± 2.76
HEC1	36.62 ± 1.12
HEC2	45.12 ± 1.40
HEC3	77.00 ± 2.80

3.1.3. Mechanical Testing

The choice of carrier appropriate for use in local periodontal treatment is crucial, as it must display sufficient mechanical strength and flexibility, be devoid of sharp edges, and be not too sticky [41,42]. The mechanical properties of rupture force and elongation at break of various CMC/GE and HEC/GE matrices were, therefore, investigated in dry states (as shown in Table 4) to determine the most appropriate matrix for clinical trials. The differences in the pore structure of matrices confer the higher flexibility of CMC scaffolds compared to HEC materials. The differences in the texture profile between CMC and HEC materials can be explained by the differences in the structure of these two polymers [43]. The matrices with a higher content of cellulose derivative elongated more, while the increase of gelatin in matrix composition decreased elongation. Increased elongation at break of matrices with a higher CMC and HEC concentration highlights the plasticizing effect of both polymers within the gelatin network [40]. Statistically significant differences were observed between all matrices with CMC sodium salt (parametric ANOVA test, $p < 0.05$) with regard to mechanical properties. It is well known that flexibility depends on the type and strength of bonds that occur between the chains building the porous matrix. Covalent bonds in a gelatin molecule are of stiff nature, so a higher content of gelatin and a higher content of amino acids affects the strength of interactions between the chains, which is reflected in a lower ratio of elongation and higher force required to tear the material apart [17]. Moreover, a homogenous, dense pore network results in strong interactions between the filler and, thus, restricts the matrix motion [40].

Table 4. Mechanical properties of CMC and HEC porous matrices: Data are presented as the mean ± SE, n ≥ 6.

Batch Code	Rupture Force (g)	Elongation at Break (%)
CMC1	251.26 ± 18.68	679.4 ± 42.83
CMC2	1345.19 ± 72.10	1027.9 ± 53.82
CMC3	2023.21 ± 48.33	918.7 ± 66.56
HEC1	469.59 ± 24.49	750.5 ± 44.12
HEC2	1007.95 ± 41.78	679.0 ± 54.13
HEC3	1647.21 ± 88.61	632.6 ± 15.26

3.2. In Vitro Drug Release

In vitro drug release was analyzed within a 120-min range. The data were plotted as a percentage cumulative release of MTZ against time, the means and SE values for MTZ–CMC and MTZ–HEC matrices are presented in Figures 6 and 7, respectively. To determine the mechanism of MTZ release from the carriers, the following mathematical models were applied: zero-order kinetics (cumulative amount of drug release versus time), first-order kinetics (log cumulative percentage of drug remaining versus time), Higuchi model (cumulative percentage of release versus square root of time), and Korsmeyer–Peppas (log cumulative percentage of drug released versus log time) equation model. The model that best fit the release data was evaluated by correlation coefficient (r^2); values for all formulations according to the models are given in Table 5.

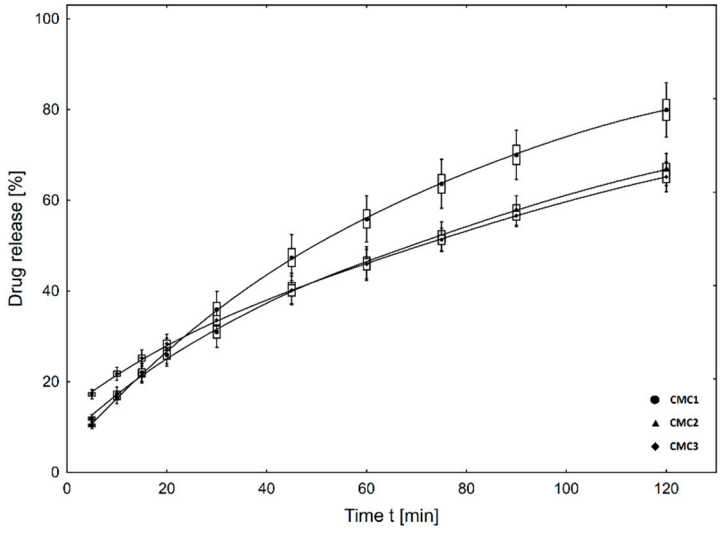


Figure 6. In vitro cumulative release profile of MTZ from matrices obtained on the basis of carboxymethyl cellulose sodium salt: Results represent mean ± SE, n = 6.

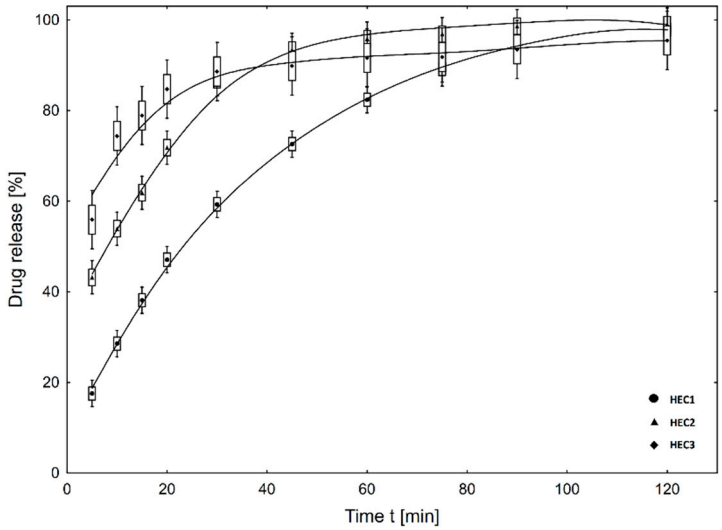


Figure 7. In vitro cumulative release profile of MTZ from matrices obtained on the basis of hydroxyethyl cellulose: Results represent mean ± SE, n = 6.

Table 5. Mathematical models and equations.

Batch Code	First-Order Kinetic Model $lnQ=lnQ_0-k\cdot t$	Zero-Order Kinetic Model $Q=Q_0-k\cdot t$	Higuchi Model $Q=k\cdot\sqrt{t}$	Korsmeyer–Peppas Model $Q=k\cdot t^n$
CMC1	$\ln Q = 4.56 - 0.013\cdot t$ $r^2 = 0.999$	$Q = 86.07 - 0.614\cdot t$ $r^2 = 0.960$	$Q = 7.06\cdot\sqrt{t}$ $r^2 = 0.974$	$Q = 3.70\cdot t^{0.656}$ $r^2 = 0.997$
CMC2	$\ln Q = 4.49 - 0.008\cdot t$ $r^2 = 0.997$	$Q = 84.96 - 0.470\cdot t$ $r^2 = 0.969$	$Q = 5.897\cdot\sqrt{t}$ $r^2 = 0.995$	$Q = 4.99\cdot t^{0.543}$ $r^2 = 0.999$
CMC3	$\ln Q = 4.43 - 0.007\cdot t$ $r^2 = 0.998$	$Q = 80.80 - 0.411\cdot t$ $r^2 = 0.979$	$Q = 6.02\cdot\sqrt{t}$ $r^2 = 0.987$	$Q = 8.21\cdot t^{0.423}$ $r^2 = 0.994$
HEC1	$\ln Q = 4.46 - 0.025\cdot t$ $r^2 = 0.969$	$Q = 70.20 - 0.698\cdot t$ $r^2 = 0.873$	$Q = 9.94\cdot\sqrt{t}$ $r^2 = 0.965$	$Q = 8.28\cdot t^{0.549}$ $r^2 = 0.974$
HEC2	$\ln Q = 3.85 - 0.031\cdot t$ $r^2 = 0.918$	$Q = 41.20 - 0.454\cdot t$ $r^2 = 0.703$	$Q = 11.76\cdot\sqrt{t}$ $r^2 = 0.225$	$Q = 29.75\cdot t^{0.276}$ $r^2 = 0.931$
HEC3	$\ln Q = 3.22 - 0.015\cdot t$ $r^2 = 0.836$	$Q = 26.65 - 0.236\cdot t$ $r^2 = 0.573$	$Q = 11.85\cdot\sqrt{t}$ $r^2 = -4.11$	$Q = 51.21\cdot t^{0.141}$ $r^2 = 0.827$

The best fit with higher correlation was found with the first-order (r^2 0.836–0.999) and the Korsmeyer–Peppas equations (r^2 0.827–0.999). For matrices CMC1, CMC2, and HEC1, the values of the release exponents (n) were found to range between 0.55 and 0.66, indicating non-Fickian (anomalous) drug release behavior. For CMC3, HEC2, and HEC3, the slope values were less than 0.5, indicating that the drug release mechanism from the tested matrices was diffusion-controlled [44,45].

When the polymeric, drug-loaded matrix comes into contact with water, swelling and relaxation of the polymer chain take place. Penetration of the solvent into the polymer matrix leads to its swelling and diffusion of the drug from the polymer-based composites. Drug release then occurs through the spaces or channels within the polymer network as well as through the dissolution and/or the disintegration of the matrix. Therefore, the mechanism of MTZ release from the matrices can be explained by simultaneously occurring phenomena: the absorption of water and the controlled diffusion of water through the matrix. The existence of the molecular relaxation process in addition to diffusion is believed to be responsible for the observed anomalous non-Fickian transport of the drug.

The results obtained for all formulations were tested by relying on a model consistent with the first-order kinetics of semi-releasing times according to the formula T 50% = ln (2)/K, which were then compared using the parametric ANOVA test together with the post hoc NIR test. A statistical analysis showed statistically significant differences in the release rate of MTZ from the compared dressings (Figure 8, Table 6). MTZ was released from hydroxyethyl cellulose-based dressings most rapidly. The mean T50% values for HEC1, HEC2, and HEC3 were 15.6 ± 4.8, 14.3 ± 3.1, and 43.0 ± 2.8, respectively. For dressings containing carboxymethyl cellulose sodium salt, the mean average durations were significantly higher: 52.3 ± 3.3 for CMC1, 82 ± 2.7 for CMC2, and 92.6 ± 2.5 for HEC1.

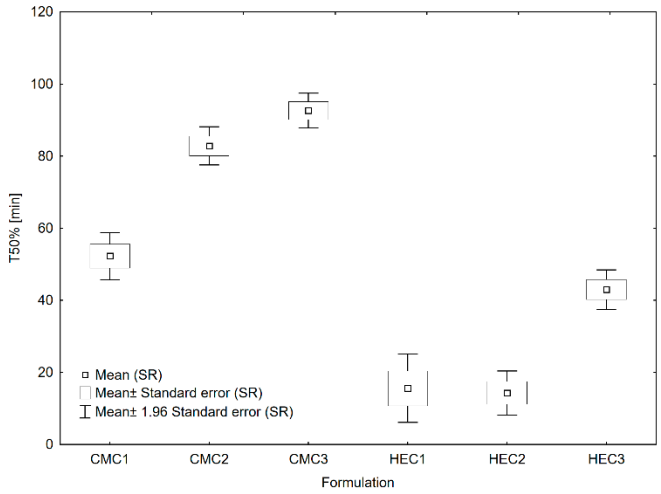


Figure 8. T50% (min) values for matrices tested.

Table 6. Comparison of the release rate of metronidazole from the tested formulations (ANOVA test, post hoc NIR test).

Batch Code	ANOVA: F = 98.9, df = 30, $p = 1.04 \times 10^{-17}$ (Significance Level $\alpha = 0.05$)					
	CMC1	**CMC2**	**CMC3**	**HEC1**	**HEC2**	**HEC3**
CMC1		3.22×10^{-7}	1.27×10^{-9}	9.30×10^{-9}	4.55×10^{-9}	5.59×10^{-2}
CMC2	3.22×10^{-7}		4.45×10^{-2}	5.39×10^{-15}	3.26×10^{-15}	1.67×10^{-9}
CMC3	1.27×10^{-9}	4.45×10^{-2}		1.42×10^{-16}	9.03×10^{-17}	1.12×10^{-11}
HEC1	9.30×10^{-9}	5.39×10^{-15}	1.42×10^{-16}		7.85×10^{-1}	2.07×10^{-6}
HEC2	4.55×10^{-9}	3.26×10^{-15}	9.03×10^{-17}	7.85×10^{-1}		9.58×10^{-7}
HEC3	5.59×10^{-2}	1.67×10^{-9}	1.12×10^{-11}	2.07×10^{-6}	9.58×10^{-7}	

3.3. Evaluation of Cytotoxic Properties of Matrices with Regard to Fibroblast and Osteoblast Reference Cell Cultures

The cytotoxicity values of matrices which did not contain metronidazole (CMC2/C and HEC2/C) were 27.9% and 25.4%, respectively. Thus, according to a binding standard, their cytotoxicity with regard to fibroblast and osteoblast cell lines would be estimated as "average". However, when the same type of matrices but supplemented with metronidazole was applied, the cytotoxicity level was high for both types of matrices (above 70% for osteoblasts and fibroblasts) according to the ISO 10,993 standard. It should be noted that no adverse effects were displayed by metronidazole-containing matrices applied clinically and that such a discrepancy between in vitro and in vivo results are common and potentially a result of unsuitable model systems currently in place.

3.4. Metronidazole Disk Diffusion Test

With regard to microbiology antimicrobial activity in the metronidazole diffusion test, the application of both types of matrices correlated with strong inhibition zones of Bacteroide growth. The mean values of this parameter were 30.7 ± 0.64 and 51.7 ± 0.64 mm for the CMC2 and HEC2 matrices, respectively. These results are consistent with the data obtained in the pharmaceutical availability assay, which shows that more metronidazole is released from HEC2 than from CMC2 matrices (Figures 5 and 6). As expected, the CMC2/C and HEC2/C control (without drug) matrices did not show bacterial activity.

3.5. Clinical Pilot Study

A decrease in all tested parameters was observed as a result of MTZ-loaded matrix application as well as after only nonsurgical treatment (Table 7). The most clinically desired effect of periodontal

treatment is a decrease in periodontal pockets depth and a decrease in bleeding indices during periodontal pockets examination. This is a result of a reduced level of inflammation, which is triggered by periopatogenic bacteria present in the periodontal pockets. The application of metronidazole-loaded matrice to the pockets correlated with a significant decrease in their depth (nonparametric Friedman's ANOVA test) (Table 8).

Table 7. Clinical pilot study results. API - Approximal Plaque Index, BOP—Bleeding on Probing, PBI—Papilla Bleeding Index.

	Test 1	Test 2	Test 3
Mean API	54	32	26
mean BOP	25	20	16
mean PBI	3.14	1.71	1.21

Table 8. The Friedman ANOVA Test.

Friedman ANOVA and Kendall Coeff of Concordance ANOVA Chi Sqr (n = 84, df = 4) = 231.032 p = 0.0000, Coeff of Concordance = 0.69057, Aver Rank r = 0.68684				
Variable	**Average Rank**	**Sum of Ranks**	**Mean**	**Std Dev**
Pocket depth	3.089286	259.5000	4.88095	2.39681
No.	4.767857	400.5000	42.50000	24.39262
Pretest	3.089286	259.5000	4.88095	2.39681
After 1 week	2.244048	188.5000	4.33333	2.16952
After 4 weeks	1.809524	152.0000	3.98810	1.94809

ANOVA, analysis of variance; Coeff, coefficient; Chi Sqr, chi-square; Std Dev, standard deviation.

The subgingival application of metronidazole-loaded matrix did not result in any negative side effects. No concern was raised by any of the patients with regards to the applied treatment. No negative reactions were observed. In the samples of 2 patients from the test group, no genetic material of *Porphyromonas gingivalis* was identified by PCR. In the other patients, each collected sample contained the pathogenic DNA. After the single application of metronidazole, the eradication of bacteria from the periodontal pockets was not successful. However, there was an observable difference noted in the color intensity of the test strap from the second test (after 7 days) compared to the first and third tests (after 1 month). To confirm these observations, a quantitative PCR should be performed.

4. Discussion

In the present study was evaluated physicochemical and biological properties of metronidazole-loaded polymer matrices. Based on the obtained results, formulation with HEC was chosen for clinical assessment after one month as an adjunct to scaling and root planning in the management of periodontitis. In pilot-study mean pocket depth after one week and four weeks, the durations of the study were 4.33 ± 2.16 mm and 3.98 ± 1.94 mm, respectively, for the test group (Table 8). Mean reduction in pocket depth from baseline were 0.55 ± 0.76 mm and 0.90 ± 0.89 mm for the duration of the study at one week and four weeks, respectively. Our results are in accordance with those of Rodrigues et al. [46] and Grover et al. [47], who found a statistically significant difference in mean pocket depth reduction between the scaling and root planning group and chlorhexidine chip-treated group. Reductions in the bleeding index score at the one-week and four-week intervals were 5.0 ± 0.65 and 9.0 ± 0.77, respectively, for the test group as compared with baseline (Table 7). There was a statistically significant difference in the bleeding index score observed at one week and four weeks compared with baseline. These findings are in accordance with those of Azmak et al., who found a mean reduction in bleeding index score at one month compared with baseline after application of controlled-release delivery of chlorhexidine gluconate.

Chaturvedi et al. [48] compared clinical effects of topical application of metronidazole-coated nanofibers in periodontal pockets as an adjunct to scaling and root planning in periodontitis on a 7-patient group. The mean reductions of pocket depth after two weeks in that study were 1.8 mm and 2.4 mm in scaling alone and scaling in combination with adjuncted metronidazole-coated nanofibers, respectively. However, our matrices offer advantages such as biodegradability, high biocompatibility, mucoadhesive properties, hemostatic properties, lack of organic solvents used to preparing, and comfortable application in comparison to other synthetic drug carriers, i.e., nanofibers.

In summary, we conclude that the in-pocket application of metronidazole is a worthwhile supplementation of the classical periodontal inflammation treatment and a feasible alternative to the use of antibiotics in periodontal diseases. As the single application of MTZ results in improvement of the clinical condition are comparable to the standard method, further research is recommended in order to test other treatment protocols.

Limitations of Pilot Study

A potential limitation of our research is that the choice of sample trials is not strictly random. Group of patients and observation time are limited. The pilot studies evaluate multiple aspects of workability of the study protocol, which are investigated so that potential bumps in the road can be dealt with before embarking upon a full-strength clinical trial.

5. Conclusions

- Metronidazole-loaded matrices based on gelatin and CMC or HEC synthesized by whipping and lyophilization methods were soft, porous, and swellable in water.
- Both matrices based on hydroxyethyl cellulose (CMC2) and hydroxyethyl cellulose (HEC2) containing metronidazole showed effective antimicrobial activity in vitro.
- No adverse effects were displayed by the metronidazole-containing matrix based on HEC applied clinically, and its single application lead to positive clinical outcomes.
- Intra-pocket application of metronidazole in the designed matrix is a worthwhile supplementation of the classical periodontal inflammation treatment and a feasible alternative to the use of antibiotics in periodontal diseases.
- Based on the elaborated pilot study, it can be concluded that the performance of the main clinical study is feasible and may bring high added value to local treatment of periodontal diseases.

Author Contributions: Conceptualization, B.K. and D.K.; methodology, B.K. and D.K.; validation, B.K. and D.K.; formal analysis, D.M. and D.K.; investigation, D.K., A.J., M.S., A.S.-J., I.D., and A.S.-J.; resources, B.K.; writing—original draft preparation, B.K. and D.K.; writing—review and editing, D.K. and B.K.; visualization, D.K. and B.K.; supervision, B.K.; project administration, B.K.

Funding: This research received no external funding.

Conflicts of Interest: The authors declare no conflict of interest.

References

1. Dusane, J.; Vrushali, M.; Borse, P.; Thakare, P.; Kshirsagar, S. Recent Trends in Treatment of Periodontitis. *Pharm. Biol. Eval.* **2016**, *3*, 19–31.
2. Graziani, F.; Karapetsa, D.; Alonso, B.; Herrera, D. Nonsurgical and surgical treatment of periodontitis: How many options for one disease? *Periodontol. 2000* **2017**, *75*, 152–188. [CrossRef]
3. Renvert, S.; Wikström, M.; Dahlén, G.; Slots, J.; Egelberg, J. On the inability of root debridement and periodontal surgery to eliminate actinobacillus actinomycetemcomitans from periodontal pockets. *J. Clin. Periodontol.* **1990**, *17*, 351–355. [CrossRef]
4. Horliana, A.; Chambrone, L.; Foz, A.; Artese, H.P.C.; Rabelo, M.; Pannuti, C.M.; Romito, G.A. Dissemination of periodontal pathogens in the bloodstream after periodontal procedures: A systematic review. *PLoS ONE* **2014**, *9*, 21–23. [CrossRef]

5. Forner, L.; Larsen, T.; Kilian, M.; Holmstrup, P. Incidence of bacteremia after chewing, tooth brushing and scaling in individuals with periodontal inflammation. *J. Clin. Periodontol.* **2006**, *33*, 401–407. [CrossRef] [PubMed]
6. Lafaurie, G.I.; Mayorga-Fayad, I.; Torres, M.F.; Castillo, D.M.; Aya, M.R.; Barón, A.; Hurtado, P.A. Periodontopathic microorganisms in peripheric blood after scaling and root planing. *J. Clin. Periodontol.* **2007**, *34*, 873–879. [CrossRef] [PubMed]
7. Castillo, D.M.; Sánchez-Beltrán, M.C.; Castellanos, J.E.; Sanz, I.; Mayorga-Fayad, I.; Sanz, M.; Lafaurie, G.I. Detection of specific periodontal microorganisms from bacteraemia samples after periodontal therapy using molecular-based diagnostics. *J. Clin. Periodontol.* **2011**, *38*, 418–427. [CrossRef]
8. Renvert, S.; Wikström, M.; Dahlén, G.; Slots, J.; Egelberg, J. Effect of root debridement on the elimination of actinobacillus actinomycetemcomitans and bacteroides gingivalis from periodontal pockets. *J. Clin. Periodontol.* **1990**, *17*, 345–350. [CrossRef]
9. Soares, G.M.; Mendes, J.A.; Silva, M.P.; Faveri, M.; Teles, R.; Socransky, S.S.; Wang, X.; Figueiredo, L.C.; Feres, M. Metronidazole alone or with amoxicillin as adjuncts to non-surgical treatment of chronic periodontitis: A secondary analysis of microbiological results from a randomized clinical trial. *J. Clin. Periodontol.* **2014**, *41*, 1149–1158. [CrossRef]
10. Addy, M.; Martin, M.V. Systemic antimicrobials in the treatment of chronic periodontal diseases: A dilemma. *Oral. Dis.* **2003**, *9*, 38–44. [CrossRef]
11. Sanz, I.; Alonso, B.; Carasol, M.; Herrera, D.; Sanz, M. Nonsurgical treatment of periodontitis. *J. Evid. Based Dent. Pract.* **2012**, *12*, 76–86. [CrossRef]
12. Matesanz-Pérez, P.; García-Gargallo, M.; Figuero, E.; Bascones-Martínez, A.; Sanz, M.; Herrera, D. A systematic review on the effects of local antimicrobials as adjuncts to subgingival debridement, compared with subgingival debridement alone, in the treatment of chronic periodontitis. *J. Clin. Periodontol.* **2013**, *40*, 227–241. [CrossRef]
13. Haris, M.; Panickal, D.M. Role of metronidazole as a local drug delivery in the treatment of periodontitis: A review. *Int. J. Oral. Heal. Med. Res.* **2017**, *3*, 141–145.
14. Nair, S.C.; Anoop, K.R. Intraperiodontal pocket: An ideal route for local antimicrobial drug delivery. *J. Adv. Pharm. Technol. Res.* **2012**, *3*, 9–15.
15. Djagny, V.B.; Wang, Z.; Xu, S. Gelatin: A valuable protein for food and pharmaceutical industries: Review. *Crit. Rev. Food Sci. Nutr.* **2001**, *41*, 481–492. [CrossRef] [PubMed]
16. Young, S.; Wong, M.; Tabata, Y.; Mikos, A.G. Gelatin as a delivery vehicle for the controlled release of bioactive molecules. *J. Control. Release* **2005**, *109*, 256–274. [CrossRef] [PubMed]
17. Tylingo, R.; Gorczyca, G.; Mania, S.; Szweda, P.; Milewski, S. Preparation and characterization of porous scaffolds from chitosan-collagen-gelatin composite. *React. Funct. Polym.* **2016**, *103*, 131–140. [CrossRef]
18. Sood, A.; Granick, M.S.; Tomaselli, N.L. Wound dressings and comparative effectiveness data. *Adv. Wound Care* **2014**, *3*, 511–529. [CrossRef]
19. Selvaraj, D.; Viswanadha, V.; Elango, S. Wound dressings-a review. *BioMedicine* **2015**, *5*, 24–28.
20. Pachuau, L. Recent developments in novel drug delivery systems for wound healing. *Expert Opin. Drug Deliv.* **2015**, *12*, 1895–1909. [CrossRef]
21. Gautam, S.; Dinda, A.K.; Mishra, N.C. Fabrication and characterization of PCL/gelatin composite nanofibrous scaffold for tissue engineering applications by electrospinning method. *Mater. Sci. Eng. C* **2013**, *33*, 1228–1235. [CrossRef] [PubMed]
22. Ahmed, E.M. Hydrogel: Preparation, characterization, and applications: A review. *J. Adv. Res.* **2015**, *6*, 105–121. [CrossRef] [PubMed]
23. Bacakova, L.; Pajorova, J.; Bacakova, M.; Skogberg, A.; Kallio, P.; Kolarova, K.; Svorcik, V. Versatile application of nanocellulose: From industry to skin tissue engineering and wound healing. *Nanomaterials* **2019**, *9*, 164. [CrossRef] [PubMed]
24. Khalili, S.; Khorasani, S.N.; Saadatkish, N.; Khoshakhlagh, K. Characterization of gelatin/cellulose acetate nanofibrous scaffolds: Prediction and optimization by response surface methodology and artificial neural networks. *Polym. Sci. Ser. A* **2016**, *58*, 399–408. [CrossRef]
25. Khalili, S.; Khorasani, S.N.; Razavi, S.M.; Hashemibeni, B.; Tamayol, A. Nanofibrous scaffolds with biomimetic composition for skin regeneration. *Appl. Biochem. Biotechnol.* **2019**, *187*, 1193–1203. [CrossRef]

26. *Polish Pharmacopeia*; Office for Registration of Medicinal Products, Medical Devices and Biocidal Products: Warsaw, Poland, 2014.
27. Eskandarinia, A.; Kefayat, A.; Rafienia, M.; Agheb, M.; Navid, S.; Ebrahimpour, K. Cornstarch-based wound dressing incorporated with hyaluronic acid and propolis: In vitro and in vivo studies. *Carbohydr. Polym.* **2019**, *216*, 25–35. [CrossRef]
28. Waghmare, V.S.; Wadke, P.R.; Dyawanapelly, S.; Deshpande, A.; Jain, R.; Dandekar, P. Starch based nanofibrous scaffolds for wound healing applications. *Bioact. Mater.* **2018**, *3*, 255–266. [CrossRef]
29. Dias, A.M.; da Silva, F.G.; de Figueiredo Monteiro, A.P.; Pinzón-García, A.D.; Sinisterra, R.D.; Cortés, M.E. Polycaprolactone nanofibers loaded oxytetracycline hydrochloride and zinc oxide for treatment of periodontal disease. *Mater. Sci. Eng. C* **2019**, *103*, 109798. [CrossRef]
30. Papapanou, P.N.; Sanz, M.; Buduneli, N.; Dietrich, T.; Feres, M.; Fine, D.H.; Flemmig, T.F.; Garcia, R.; Giannobile, W.V.; Graziani, F. Periodontitis: Consensus report of workgroup 2 of the 2017 World Workshop on the classification of periodontal and peri-implant diseases and conditions. *J. Clin. Periodontol.* **2018**, *45*, S162–S170. [CrossRef]
31. Lange, D.E.; Plagmann, H.C.; Eenboom, A.P.A. Klinische Bewertungsverfahren zur Objektivierung der Mundhygiene. *Dtsch. Zahnarztl.* **1977**, *32*, 44–47.
32. Ainamo, J.; Bay, I. Problems and proposals for recording gingivitis and plaque. *Int. Dent. J.* **1975**, *25*, 229–235.
33. Saxer UPMühlemann, H.R. Motivation und Aufklärung. *Schweiz. Mschr. Zahnheilk.* **1975**, *85*, 905–1002.
34. Domínguez, L.; Cepeda, J.; Sánchez, L.; Márquez, R.; Aranda Romo, S. Evaluation of the clinical effect of a probiotic mouthwash in the treatment of generalized marginal chronic gingivitis. Randomized pilot study. *J. Oral. Res.* **2018**, *7*, 134–140. [CrossRef]
35. García-Gargallo, M.; Zurlohe, M.; Montero, E.; Alonso, B.; Serrano, J.; Sanz, M.; Herrera, D. Evaluation of new chlorhexidine- and cetylpyridinium chloride-based mouthrinse formulations adjunctive to scaling and root planing: Pilot study. *Int. J. Dent. Hyg.* **2017**, *15*, 269–279. [CrossRef] [PubMed]
36. Mombelli, A. Microbial colonization of the periodontal pocket and its significance for periodontal therapy. *Periodontol. 2000.* **2018**, *76*, 85–96. [CrossRef] [PubMed]
37. Mapstone, N.P.; Lynch, D.A.; Lewis, F.A.; Axon, A.T.; Tompkins, D.S.; Dixon, M.F.; Quirke, P. Identification of Helicobacter pylori DNA in the mouths and stomachs of patients with gastritis using PCR. *J. Clin. Pathol.* **1993**, *46*, 540–543. [CrossRef] [PubMed]
38. Orrù, G.; Marini, M.F.; Ciusa, M.L.; Isola, D.; Cotti, M.; Baldoni, M.; Piras, V.; Pisano, E.; Montaldo, C. Usefulness of real time PCR for the differentiation and quantification of 652 and JP2 Actinobacillus actinomycetemcomitans genotypes in dental plaque and saliva. *BMC Infect. Dis.* **2006**, *6*, 98. [CrossRef]
39. Radwan-Oczko, M.; Jaworski, A.; Duś, I.; Plonek, T.; Szulc, M.; Kustrzycki, W. Porphyromonas gingivalis in periodontal pockets and heart valves. *Virulence* **2014**, *5*, 575–580. [CrossRef]
40. Kanimozhi, K.; Khaleel Basha, S.; Sugantha Kumari, V. Processing and characterization of chitosan/PVA and methylcellulose porous scaffolds for tissue engineering. *Mater. Sci. Eng. C* **2016**, *61*, 484–491. [CrossRef]
41. Labib, G.S.; Aldawsari, H.M.; Badr-Eldin, S.M. Metronidazole and pentoxifylline films for the local treatment of chronic periodontal pockets: Preparation, in vitro evaluation and clinical assessment. *Expert Opin. Drug Deliv.* **2014**, *11*, 1981. [CrossRef]
42. Morales, J.O.; McConville, J.T. Manufacture and characterization of mucoadhesive buccal films. *Eur. J. Pharm. Biopharm.* **2011**, *77*, 187–199. [CrossRef] [PubMed]
43. Petchsomrit, A.; Sermkaew, N.; Wiwattanapatapee, R. Hydroxypropylmethyl cellulose-based sponges loaded self-microemulsifying curcumin: Preparation, characterization, and in vivo oral absorption studies. *J. Appl. Polym. Sci.* **2016**, *133*, 1–10. [CrossRef]
44. Thakur, G.; Singh, A.; Singh, I. Chitosan-montmorillonite polymer composites: Formulation and evaluation of sustained release tablets of aceclofenac. *Sci. Pharm.* **2016**, *84*, 603–617. [CrossRef] [PubMed]
45. Basak, S.C.; Kumar, K.S.; Ramalingam, M. Design and release characteristics of sustained release tablet containing metformin HCl. *Rev. Bras. Ciencias. Farm. J. Pharm. Sci.* **2008**, *44*, 477–483. [CrossRef]
46. Rodrigues, I.F.; Machion, L.; Casati, M.Z.; Nociti, F.H.; Toledo, S., Jr.; Sallum, A.W.; Sallum, E.A. Clinical evaluation of the use of locally delivered chlorhexidine in periodontal maintenance therapy. *J. Periodontol.* **2007**, *78*, 624–628. [CrossRef]

47. Grover, V.; Kapoor, A.; Malhotra, R.; Battu, V.S.; Bhatia, A.; Sachdeva, S. To assess the effectiveness of a chlorhexidine chip treatment of chronic periodontitis: A clinical and radiographic study. *J. Indian. Soc. Periodontol.* **2011**, *15*, 139–146. [CrossRef]
48. Chaturvedi, T.P.; Srivastava, R.; Srivastava, A.K.; Gupta, V.; Verma, P.K. Evaluation of metronidazole nanofibers in patients with chronic periodontitis: A clinical study. *Int. J. Pharm. Investig.* **2012**, *2*, 213–217.



© 2019 by the authors. Licensee MDPI, Basel, Switzerland. This article is an open access article distributed under the terms and conditions of the Creative Commons Attribution (CC BY) license (http://creativecommons.org/licenses/by/4.0/).